Revealing the action mechanisms of scutellarin against glioblastoma based on network pharmacology and experimental validation

Junzhao SUN[1#], Hongwei WANG[1#], Gang CHENG[1], Leiming ZHANG[2], Zhifeng QU[2], Chengchen HAN[1],
Wei ZHENG[3], Lin WU[2], Jianning ZHANG[1*] (iD)

Abstract
Scutellarin, a flavonoid compound found in *Scutellaria barbata*, has been demonstrated to exert anti-cancer property in a variety of human malignancies. However, its biological significance and underlying mechanism in glioblastoma (GBM) remain ambiguous. Network pharmacology approaches and molecular docking technologies were used to predict the crucial biological processes, candidate targets and signaling pathways of scutellarin against GBM. CCK-8, EdU, and colony formation experiments were performed to determine the effects of scutellarin on cell proliferation. Flow cytometry analysis was utilized to detect apoptosis. Western blot assays were used to measure the expression of proteins associated with EGFR-PI3K-AKT signaling. Through network pharmacology and molecular docking analysis, we found that EGFR might be a potential target and PI3K-AKT signaling might be the key signaling pathway for scutellarin to combat GBM. Scutellarin inhibited cell proliferation and induced apoptosis in a dose-dependent manner. Scutellarin also suppressed the phosphorylation level of EGFR in a dose-dependent manner. Scutellarin inactivated PI3K-AKT signaling by targeting EGFR. Moreover, scutellarin-mediated suppression of cell proliferation and increase of apoptosis was greatly reversed in GBM after overexpressing EGFR. Taken together, scutellarin is a novel inhibitor of EGFR-PI3K-AKT signaling to prevent GBM progression.

Keywords: network pharmacology; scutellarin; glioblastoma; EGFR-PI3K-AKT.

Practical Application: Scutellarin exerts inhibitory effects on glioblastoma progression.

1 Introduction

Glioblastoma (GBM) is the most common and aggressive primary tumor of the central nervous system (CNS), accounting for 47.1% of all malignant brain tumors (Thakkar et al., 2014). The incidence of GBM is increased with age, with 13.16 cases per 100,000 population from 2000 to 2017 (Chen et al., 2021). Due to high invasiveness and relapse rate, GBM patients usually have a dismal prognosis, with the five-year and ten-year survival rate is merely 5.5% and 0.71% (Ostrom et al., 2017; Tykocki & Eltayeb, 2018). Despite that surgery resection followed by radiochemotherapy has improved the survival rate of GBM patients, serious adverse reactions and drug resistance greatly limit their clinical efficacy (Zanders et al., 2019; Peng et al., 2020). GBM patients can only obtain a modest 14-month overall median survival period after diagnosis (Delgado-López & Corrales-García, 2016). Thus, developing effective anti-cancer drugs with low toxicity as alternative treatments becomes a trend.

Traditional Chinese medicine (TCM) has gained increasing attention in human cancers with the characteristic of multiple-targets and less toxicity (Hanachi et al., 2020; Zhou et al., 2021). Natural products have been reported to exert physiological effects in GBM by regulating signaling pathways associated with cell viability, apoptosis, migration/invasion, angiogenesis,

and chemoresistance (Abbas et al., 2020; Erices et al., 2018). Scutellarin, an flavonoid glucuronide from *Erigeron breviscapus*, is demonstrated to possess multiple pharmacological activities, such as anti-oxidant, anti-inflammation, vascular relaxation, anti-platelet, anti-coagulation, and myocardial protection (Wang & Ma, 2018). Scutellarin is found to exert anti-cancer properties by modulating cell proliferation, apoptosis, autophagy, migration, invasion, adhesion, and angiogenesis in various malignancies, such as esophageal cancer (Liu et al., 2019a), non-small cell lung cancer (Sun et al., 2018), melanoma (Li et al., 2019), colorectal cancer (Xiong et al., 2020), gastric cancer (Li et al., 2021), hepatocellular carcinoma (Liu et al., 2019b), and breast cancer (Hou et al., 2017). A previous document revealed that scutellarin inhibited cell metastasis and chemoresistance in glioma *in vitro* (Tang et al., 2019). However, the detailed action targets and molecular mechanisms of scutellarin against GBM remain unclear.

Network pharmacology, an emerging discipline intergrating bioinformatics, systems biology, and pharmacology, is of great help to rational and cost-effective drug development. Network pharmacology aims to construct a comprehensive "drug-target-disease" model by analyzing the biological network and screening

out the nodes of particularly interest (Hao & Xiao, 2014). Network pharmacology approach has been regarded as a powerful tool to reveal the molecular mechanism of Traditional Chinese Medicine (TCM) and natural compounds in human diseases (Kibble et al., 2015; Yuan et al., 2017). In the current study, we used a network pharmacology method to explore the key targets, biological functions and associated pathways of scutellarin to treat GBM. Then, we performed *in vitro* experiments to confirm the the proposed effects and mechanisms of scutellarin as an anti-GBM agent.

2 Materials and methods

2.1 Differentially expressed genes (DEGs) analysis

The GSE108474 datasets containing 221 GBM tumor tissues and 28 normal brain tissues were downloaded from the GEO database (Clough & Barrett, 2016). The DEGs were displayed as volcano plot. The DEGs with adjusted $P < 0.05$ and $|log2Fold Change (FC)| \geq 1$ were considered statistically significant. The DEGs with adjusted $P < 0.05$ and $|log2Fold Change (FC)| \geq 2$ were also presented as heat map by a freely available web server heatmapper (Babicki et al., 2016).

2.2 Collection of targets related to scutellarin

The potential targets of scutellarin were collected by using PharmMpper (Wang et al., 2017) with normal fit score > 0.3, TargetNet (Yao et al., 2016) with probability > 0, and SwissTargetPrediction (Daina et al., 2019) with probability > 0. After deleting the duplicates, we obtained the putative targets of scutellarin.

2.3 Genes associated with GBM and scutellarin

The common targets of GBM and scutellarin were presented in the form of a venn diagram. The expression difference of overlapping genes were displayed by a heat map.

2.4 Network establishment

The Protein-Protein Interaction (PPI) network of overlapping genes was constructed using String database (Szklarczyk et al., 2017) and visualized by Cytoscape 3.7.2 software. The CytoNCA plugin in Cytoscape was used to screen the key genes in PPI network. The Molecular Complex Detection (MCODE) plugin in Cytoscape was used to analyze the clustered modules in the scutellarin-disease PPI network.

2.5 GO and KEGG pathway enrichment

DAVID (Huang et al., 2007) was applied to reveal the GO function and KEGG pathway enriched in the key targets of scutellarin against GBM. The significant GO and pathway terms with $P < 0.05$ was presented as bar graph or bubble chart.

2.6 Molecular docking

The three-dimensional (3D) structures of scutellarin molecule were obtained from PubChem dababase and saved as a PDB format.

The protein crystal structures of EGFR and RAF1 (PDBcode: 4LL0, 6VJJ) were retrieved from the RCSB PDB database. Then, the protein structure was prepared by using PyMOL software to remove water molecules and heteromolecules. The AutoDock Vina was utilized to perform the molecular docking and calculate the predicted binding energy (kcal/mol).

Pymol and LigPlos software was used for the visualization of results.

2.7 Cell culture

Human GBM cell lines (U251 and LN229) were obtained from the Cell Bank of Chinese Academy of Sciences (Shanghai, China). Cells were maintained in DMEM (Hyclone, Logan, UT, USA) containing 10% FBS and 1% penicillin/streptomycin at 37 °C in an incubator with 5% CO_2. Scutellarin (purity > 98%) was purchased from Sigma-Aldrich (Merck KgaA, Darmstadt, Germany). EGFR-overexpression plasmid (EGFR) was obtained from RiboBio (Guangzhou, China)

2.8 Cell viability assay

Cell Counting Kit-8 (CCK-8; Dojindo, Kumamoto, Japan) was utilized to measure cell viability. U251 and LN229 cells were seeded into 96-well plates (5×10^3 cells/well). On the next day, cells were treated with scutellarin at indicated (0, 50, 100, 150, 200, 250, 300, 400, 500 and 600 µM) for 48 h. Subsequently, 10 µL of CCK-8 reagent was added for another 4 h of incubation. The absorbance at 450 nm was recorded by a microplate reader (Thermo Fisher Scientific Inc., Waltham, MA, USA) and the IC_{50} value of scutellarin was calculated.

2.9 EdU assay

To assess cell proliferation ability, the Cell-Light™ EdU DNA cell proliferation kit (RiboBio, Guangzhou, China) was used. U251 and LN229 cells were inoculated into the 96-well plates at the density of 5×10^3 cells/well. After 24 h, cells exposed with indicated concentrations of scutellarin (0, 200, 300, 400 µM) for 48 h. Then, EdU solution was added to each well at 25 µM, followed by an incubation of 2 h at 37 °C. Subsequently, cells were fixed with 4% paraformaldehyde, permeabilized with 0.5% Triton X-100, washed with PBS and treated with Apollo reaction buffer. Finally, cells were subjected to DAPI dye for 20 min at room temperature. Images were captured by a fluorescence microscope. The EdU-positive cells (%) = The count of green EdU/The count of blue DAPI × 100%.

2.10 Colony formation assay

U251 and LN229 cells were seeded onto 6-well plates at 1000 cells per well. After incubation at 37°C overnight, cells were treated with designated concentration of scutellarin (0, 200, 300, 400 µM) for 12 days, during which the medium was refreshed every 3 days. Then, cells were washed with PBS for 3 times, fixed with 4% paraformaldehyde for 15 min, and stained with 0.1% crystal violet for 30 min. The colonies with cell number greater than 50 were manually counted from three randomly selected fields.

2.11 Apoptosis assay

U251 and LN229 cells were seeded onto 6-well plates at 1×10^6 cells per well, and incubated at 37°C overnight. Then, scutellarin (0, 200, 300, 400 μM) was added to each well for another 48 h incubation. After digestion with 0.25% trypsin, cells were harvested by centrifugation at 1000 rpm for 5 min, washed with PBS and detected by Annexin V-FITC/PI apoptosis detection kit (Vazyme, Nanjing, China). Briefly, cells were resuspended in 100 μL binding buffer, followed by stained with 5 μL Annexin V-FITC and 5 μL PI at room temperature for 10 min in the dark. After adding 100 μL binding buffer, we placed the samples in the FACSCalibur flow cytometer (BD Biosciences, Franklin Lakes, NJ, USA) to determine apoptosis.

2.12 Western blot assay

After treatment with scutellarin (0, 200, 300, 400 μM) for 48 h, U251 and LN229 cells were harvested and lysed in lysis buffer (Beyotime, Shanghai, China) containing protease inhibitors. The concentration of extracted protein was determined by a BCA Protein Assay Kit (Beyotime). The protein sample (30 μg) was loaded onto 10% SDS-PAGE gels and transferred onto PVDF membranes (BioRad, Hercules, CA, USA). Then, the membranes were blocked in 5% skimmed milk for 1 h at room temperature, followed by incubation with the primary antibodies against EGFR, p-EGFR, AKT, p-AKT, PI3K, p-PI3K and GAPDH (Cell Signaling Technology, Danvers, MA, USA) at 1:1,000 overnight at 4 °C. After incubation with the appropriate secondary antibody for 1 h at room temperature, the protein bands were visualized by an enhanced chemiluminescent kit (GE Healthcare, Chicago, IL, USA). GAPDH was used as an internal reference to normalize the relative expression of proteins.

2.13 Statistical analysis

All data was presented as mean ± SD. The statistical analysis was performed with one-way analysis of variance (ANOVA) by using GraphPad Prism 9.0 software. The difference with $P < 0.05$ was considered statistically significant. All experiments were repeated at least three times.

3 Results

3.1 Identifying DEGs in GBM

GSE108474 datasets was downloaded to identify the DEGs between 221 GBM tumor tissues and 28 normal brain tissues. With $|\log_2$Fold Change (FC)$| \geq 1$ and adjusted $P < 0.05$ as screening threshold, a total of 4775 DEGs were found, in which there were 2218 up-regulated genes and 2557 down-regulated genes (Figure 1A). A total of 1249 DEGs with $|\log_2$Fold Change (FC)$| \geq 2$ and adjusted $P < 0.05$ were displayed as the heat map (Figure 1B).

3.2 Collecting targets related to GBM and scutellarin

According the data from PharmMpper, TargetNet and SwissTargetPrediction, we identified 471 genes associated with scutellarin. An online tool Venny 2.1.0 was utilized to display the intersection of scutellarin targets and GBM-related DEGs. A total of 139 overlapping genes that might be involved in scutellarin against GBM were acquired (Figure 2A). A heat map was drawn to visualize these 139 common DEGs (Figure 2B).
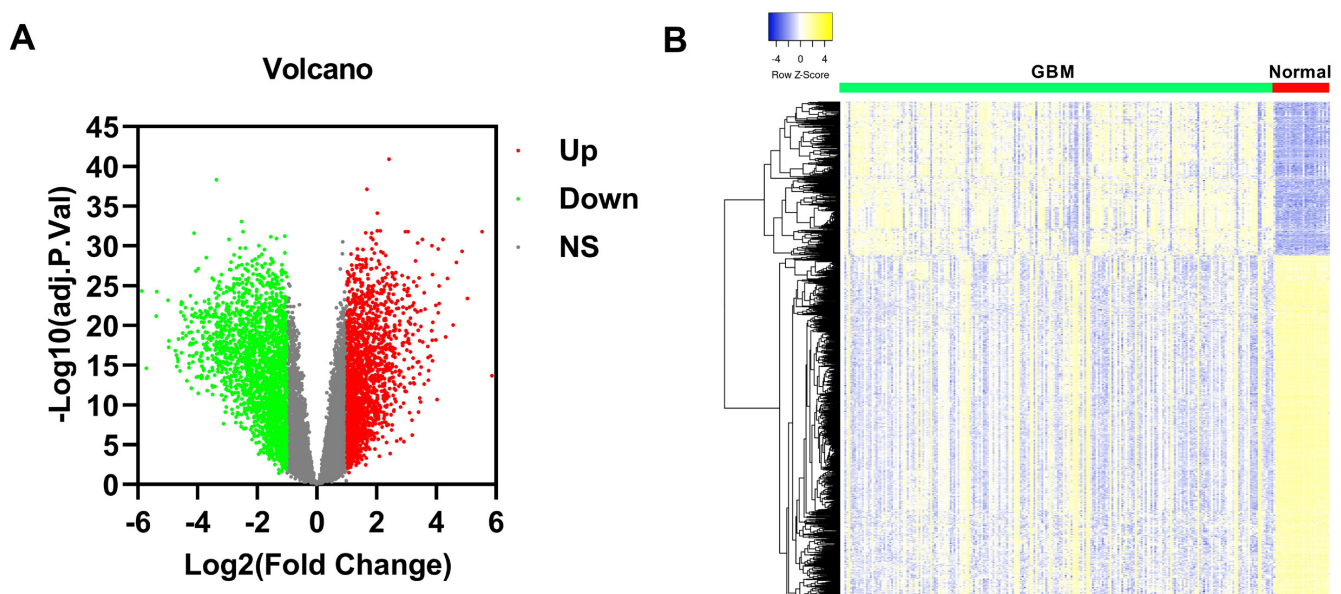

Figure 1. Volcano plot and heat map of the DEGs in GBM. (A) Volcano diagrams of DEGs in GBM. Red and green dots represent genes that are up-regulated and down-regulated in GBM tumor tissues, respectively. (B) Heat maps of GBM-related DEGs with adjusted $P < 0.05$ and |log2Fold Change (FC)| ≥ 2.

3.3 Construction and analysis of PPI network

The PPI network was established by inputting these 139 candidate biological targets into the STRING database, and analyzed with Cytoscape software. As shown in Figure 3A, there existed 130 nodes and 684 edges in this network. Then, the plugin CytoNCA in cytoscape was used to perform topology analysis.

The top 20 core nodes were screened based on the degree values from high to low (Figure 3B).

3.4 GO and KEGG pathway enrichment of core targets

DAVID was used to analyze the GO annotation and KEGG pathway of core targets. A total of 151 GO items, including
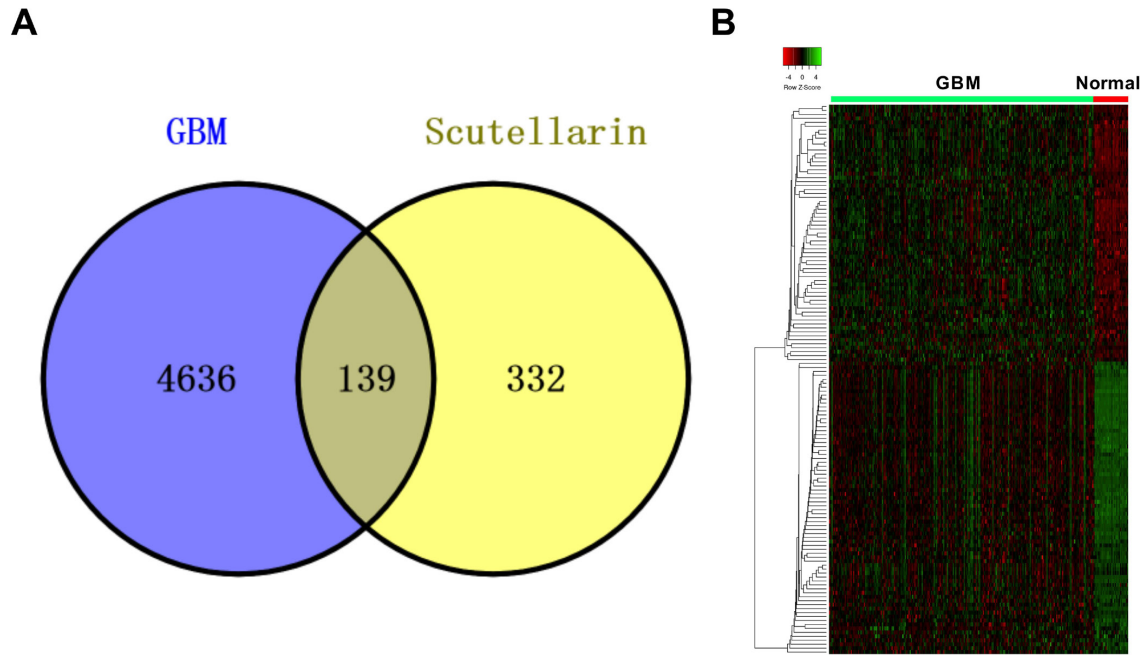

Figure 2. Identification of targets related to scutellarin and GBM. (A) Venn diagram of scutellarin targets and GBM targets. (B) Heat map of 139 common DEGs.
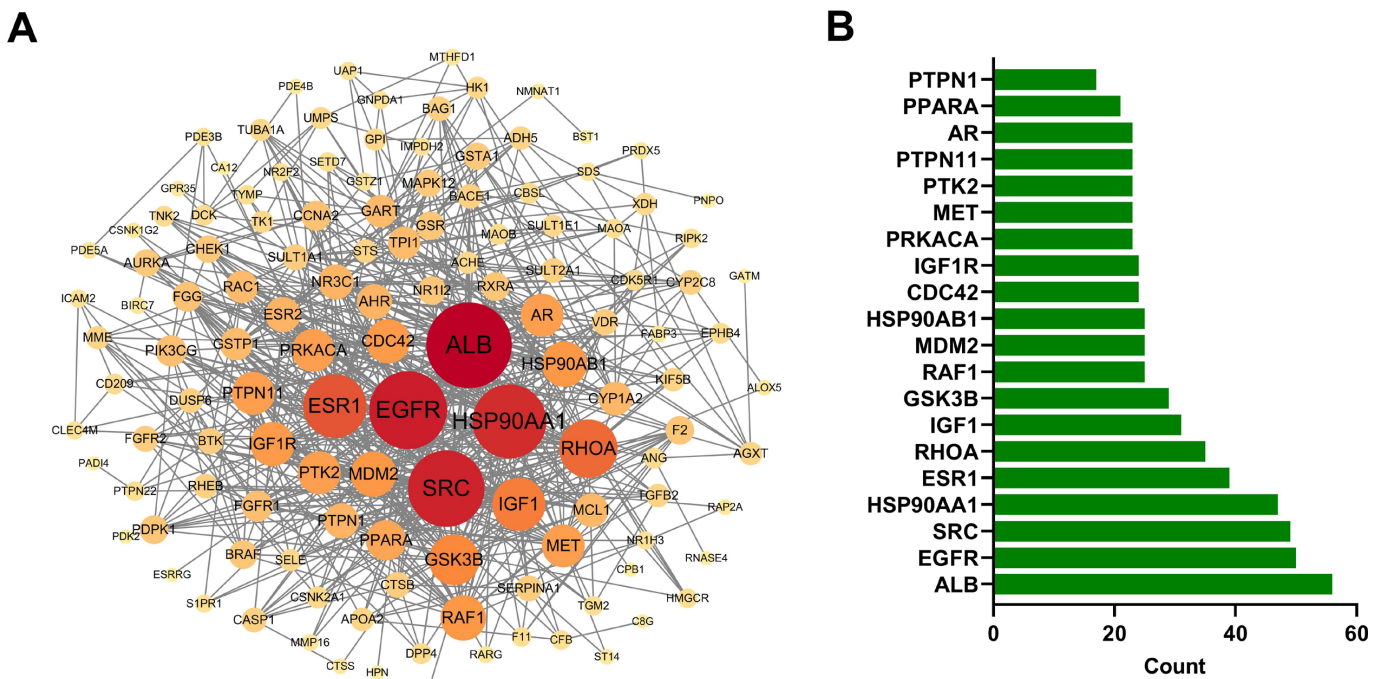

Figure 3. PPI network construction and analysis. (A) PPI network containing 130 nodes and 684 edges. The larger the node and the darker the color, the more important it is in the hub network. (B) The top 20 core targets were displayed by a bar plot.

95 biological processes (BPs), 18 cell components (CCs), and 38 molecular functions (MFs) items, were obtained with $P < 0.05$. The top ten enriched terms in BPs, CCs and MFs were shown in Figure 4A. For BPs, the candidate genes were associated with the negative regulation of apoptotic process, protein autophosphorylation, positive regulation of DNA replication and signal transduction. For CCs, the targets were mainly enriched in plasma membrane, cytosol and nucleus. For MFs, the enriched terms were protein kinase activity, protein binding and enzyme binding. KEGG analysis revealed 55 related pathways. The most significantly enriched 20 pathways were displayed as bubble charts in Figure 4B, including Pathways in cancer, PI3K-AKT signaling pathway, Ras signaling pathway, and Rap1 signaling pathway. To further the determine the molecular mechanism by which scutellarin inhibited GBM, a target-pathway network was established with the top 20 pathways and corresponding targets (Figure 4C). This network was comprised of

38 nodes (18 for proteins and 20 for pathways) and 147 edges. Among these targets, RAF1, EGFR, SRC, CDC42 and IGF1R were found as the molecules with higher degree. Among these 18 core targets, there were 10 involved in PI3K/AKT signaling pathway. EGFR, IGF1R and RAF1 were the most important targets of scutellarin to affect PI3K/AKT signaling. According to these data, we speculated that scutellarin might regulate cell proliferation and apoptosis in GBM by PI3K/AKT signaling pathway via binding with EGFR, IGF1R and RAF1.

3.5 Clustering analysis in PPI network

By using MCODE plugin in Cytoscape, we obtained two important modules in the PPI network of 139 candidate targets (Figure 5A and B). There were 17 core targets in module 1 and 11 core targets in module 2. Functionally, these targets were mainly enriched in apoptotic process, DNA replication and cell proliferation (Figure 5C and D). KEGG analysis showed that the targets in module 1 were mainly associated with Ras signaling pathway, Rap 1 signaling pathway, and PI3K-AKT signaling pathway (Figure 5E). The targets in module 2 were mainly related to PI3K-AKT signaling pathway and Ras signaling pathway (Figure 5F).

3.6 Molecular docking of scutellarin and potential targets

Based on the data from Oncomine and GEPIA, EGFR and RAF1 expression was significantly up-regulated in GBM tumor tissues compared with normal brain tissues (Figure 6A and B). Then, molecular docking was performed to elucidate the interaction between scutellarin and EGFR or RAF1. As shown in Figure 6C and D, EGFR (PDB ID: 4LL0) and RAF1 (PDB ID: 6VJJ) possesses stable binding sites in scutellarin, with the binding energy of -9.3 kcal/mol and -8.1 kcal/mol, respectively. The hydrogen bonds were the main forms of interaction between scutellarin and EGFR or RAF1.

3.7 Scutellarin represses cell proliferation and promotes apoptosis in GBM

To confirm the effects of scutellarin on GBM, U251 and LN229 cells were treated with different doses of scutellarin (0, 50, 100, 150, 200, 250, 300, 400, 500 and 600 μM) for 48 h. CCK-8 analysis revealed a dose-dependent decrease of cell viability (Figure 7A). The IC_{50} values of scutellarin were 270.6 and 296.2 μM for U251 and LN229 cells, respectively. Then, U251 and LN229 cells were cultured in medium containing scutellarin (0, 200, 300, 400 μM). EdU and colony formation assay showed that scutellarin reduced the EdU-positive cells and colony number in a dose-dependent manner (Figure 7B and C). Also, scutellarin resulted in the increase of cell apoptosis in a dose-dependent manner (Figure 7D). These data suggested the anti-tumor property of scutellarin in GBM.

3.8 Scutellarin suppresses cell proliferation and induces apoptosis in GBM by regulating EGFR-PI3K-AKT signaling pathway

Based on the data from network pharmacology, we speculated that scutellarin could inhibit the GBM progression by regulating EGFR-PI3K-AKT signaling. After treatment with scutellarin (0, 200, 300, 400 μM) for 48 h, western blot analysis was performed in U251 and LN229 cells to determine the expression of EGFR and p-EGFR. As shown in Figure 8A, the phosphorylation levels of EGFR was significantly inhibited in a dose-dependent manner, there is no evident alteration in its total expression. Moreover, scutellarin significantly suppressed the expression of p-EGFR,
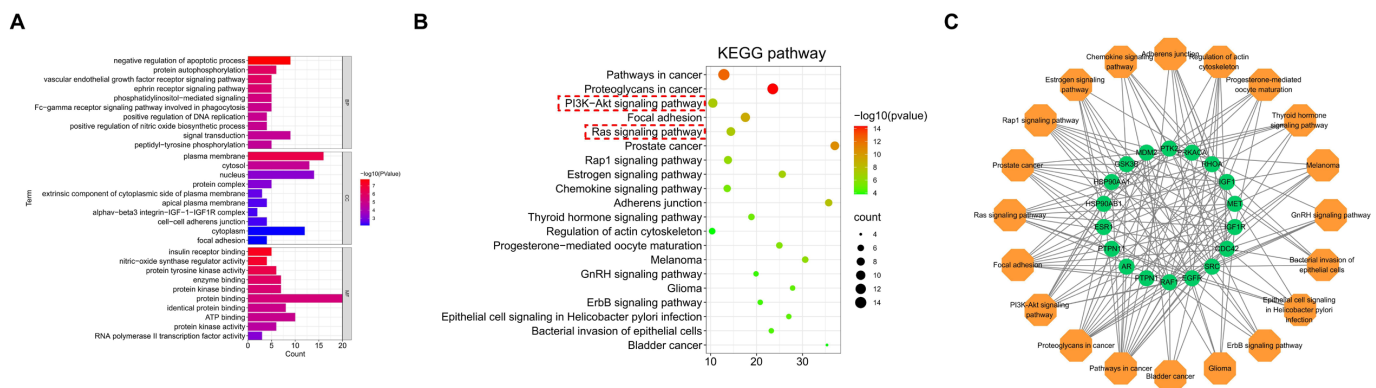

Figure 4. GO and KEGG pathway enrichment analysis of core targets. (A) Column plot showing the top 10 BPs, 10 CCs and 10 MFs. (B) Bubble chart for the top 20 KEGG pathways. (C) The target-pathway network of scutellarin against GBM.
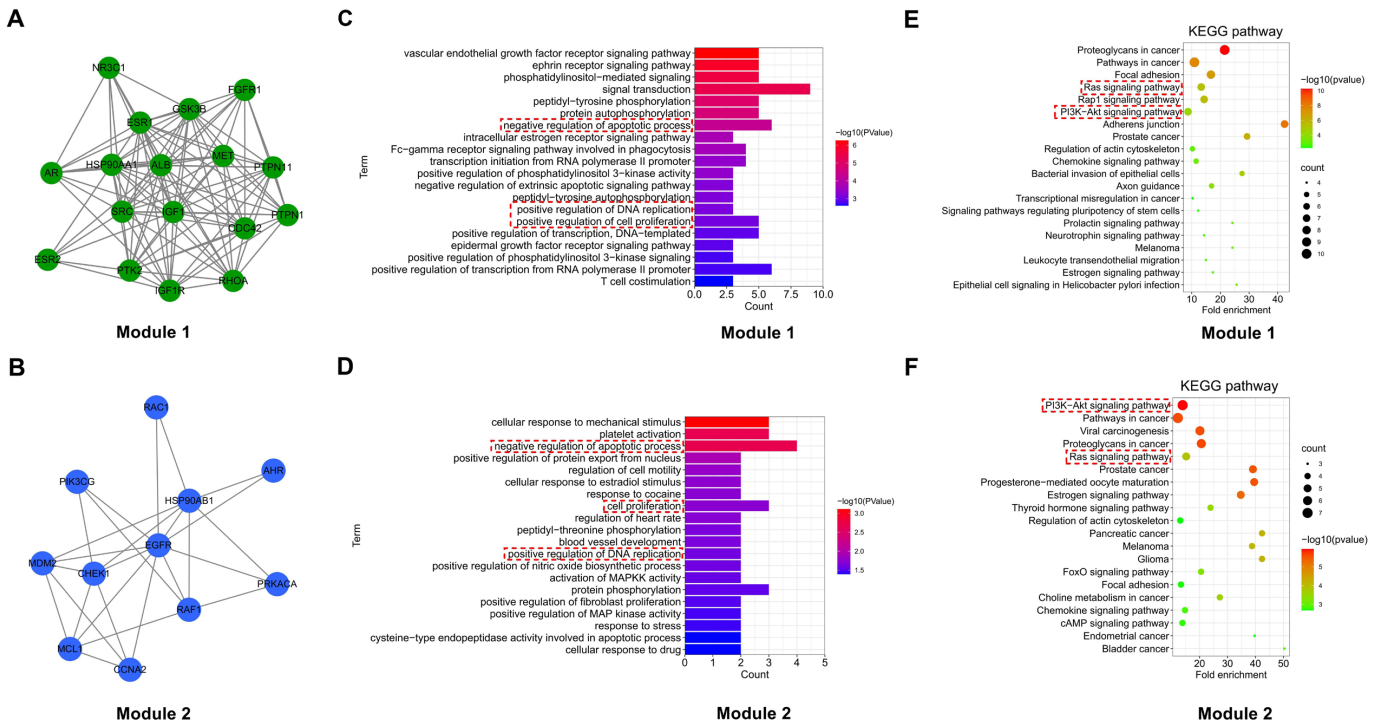
Using network pharmacology to reveal the mechanisms of scutellarin against glioblastoma

Figure 5. Cluster analysis for potential targets of scutellarin against GBM. (A and B). MCODE algorithm was used to perform cluster analysis of PPI network. (C and D) The GO-BPs analysis of core targets in module 1 and 2. (E and F) The KEGG pathway enrichment analysis of core targets in module 1 and 2.
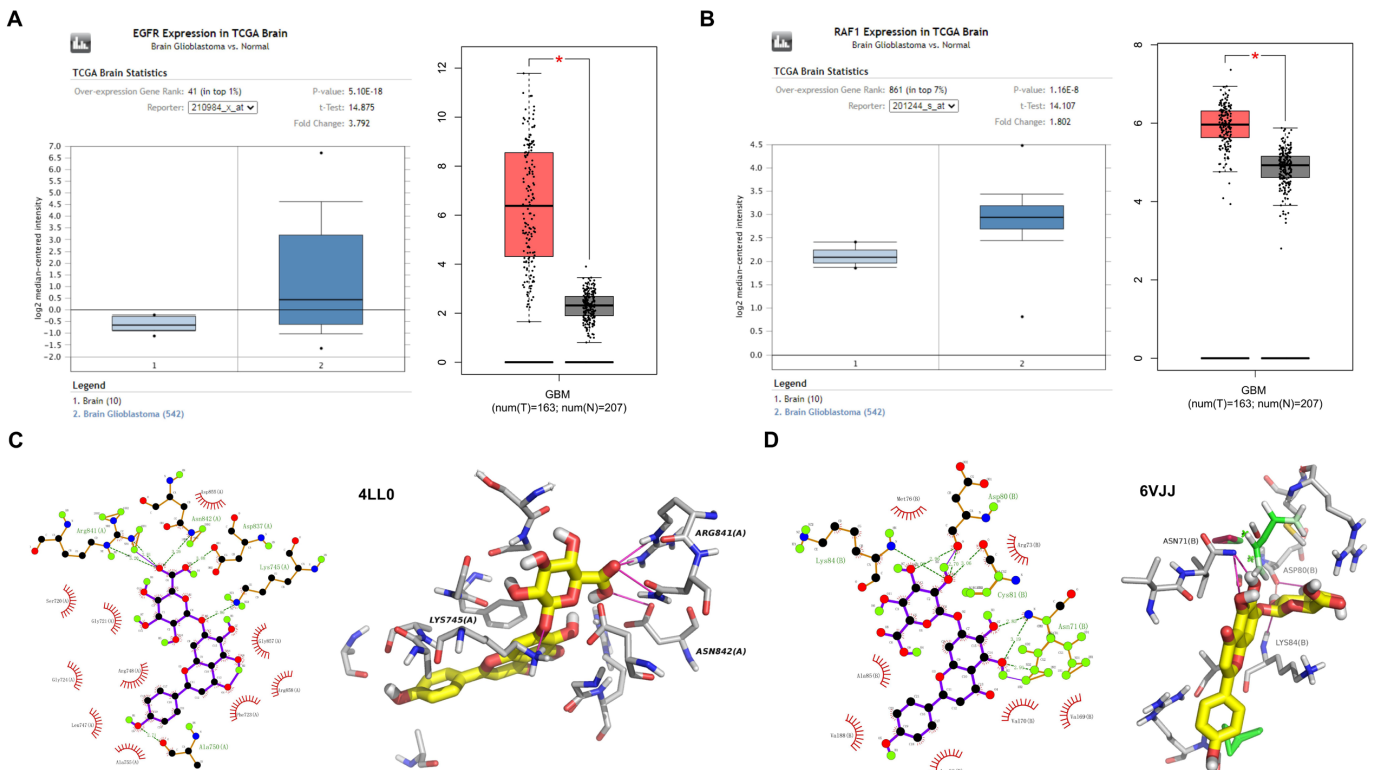

Figure 6. Molecular docking of scutellarin and its potential targets. (A and B) Expression of EGFR and RAF1 in Oncomine and GEPIA databases. (C) The 2D and 3D representation of the binding of scutellarin with EGFR (4LL0). (D) The 2D and 3D representation of the binding of scutellarin with RAF1 (6VJJ).
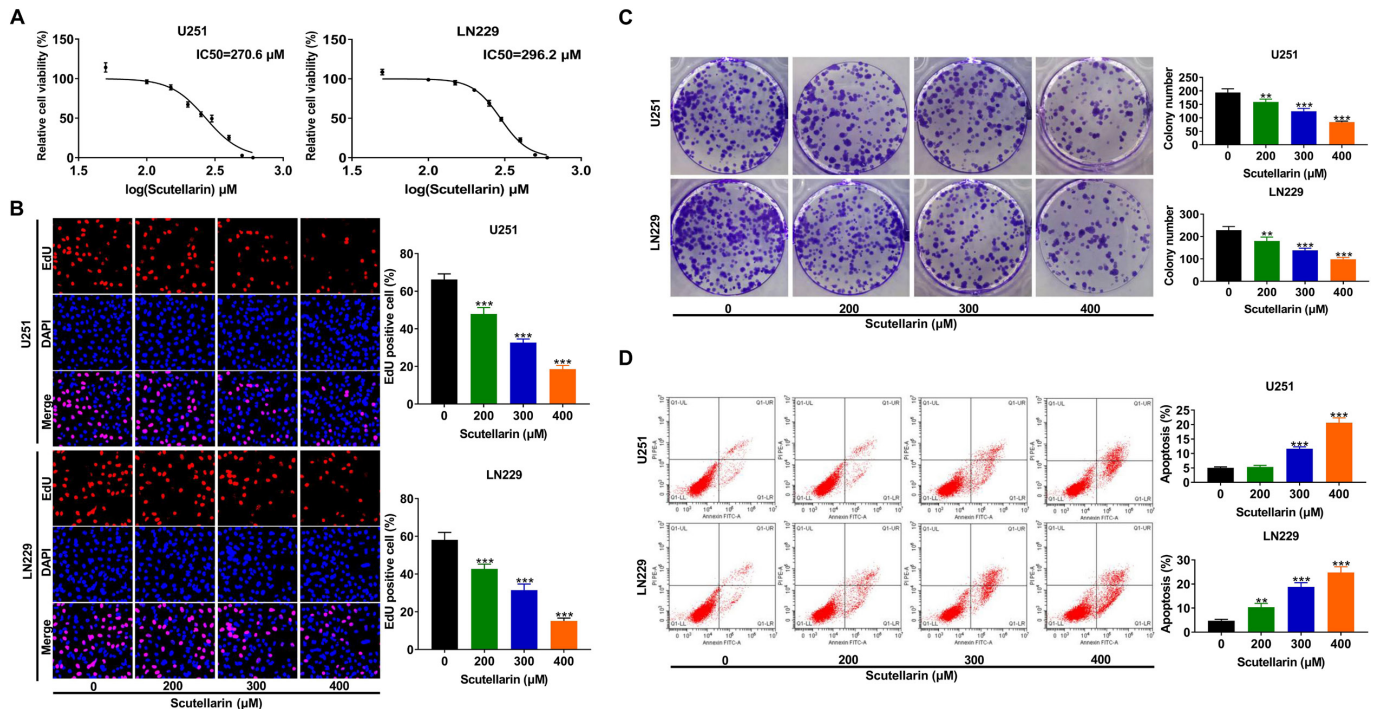
Figure 7. Scutellarin inhibits GBM cell proliferation and induces apoptosis. (A) U251 and LN229 cell viability was determined by CCK-8 assay after treatment with various concentraions of scutellarin. (B) Cell proliferation ability was measured by EdU assay in U251 and LN229 cell treated scutellarin (0, 200, 300, and 400 µM) for 48 h. (C) Colony formation assays were performed in U251 and LN229 cells after treatment with indicated doses of scutellarin (0, 200, 300, and 400 µM). (D) After treatment with scutellarin (0, 200, 300, and 400 µM) for 48 h, flow cytometry analysis was used to detect cell apoptosis. **$P < 0.01$, ***$P < 0.001$ vs. 0 µM group.

p-PI3K and p-AKT, while these effects were attenuated in GBM cells after overexpressing EGFR (Figure 8B). These data confirmed that scutellarin could inactivate PI3K-AKT signaling by targeting EGFR. Furthermore, EGFR overexpression obviously abated the inhibitory effects of scutellarin on cell viability and colony forming ability (Figure 8C and D). Also, scutellarin-induced apoptosis was effectively reversed by EGFR overexpression (Figure 8E). Taken together, scutellarin repressed GBM cell proliferation and enhanced apoptosis by inactivating EGFR/PI3K/AKT signaling pathway.

4 Discussion

GBM is one of the most aggressive intracranial malignant tumors with an dismal prognosis (Davis, 2016). Natural products have been demonstrated as useful multi-targeted therapies with minimum cytotoxicity to combat various cancers, including GBM (Dutta et al., 2019; Vengoji et al., 2018; Huang et al., 2019). In this study, we used a network pharmacology method to predict the biological functions, potential targets and mechanisms of scutellarin aganist GBM. Moreover, molecular docking simulation and *in vitro* experiments were performed to verify the targets and pathways by which scutellarin exerted anti-GBM activity.

Scutellarin, a naturally flavone glycoside, has been found to exert anti-tumor activity in different human tumors. For instance, scutellarin suppressed hypoxia-induced cell migration and invasion in bladder cancer by regulating PI3K/Akt and MAPK pathways (Lv et al., 2019). Scutellarin inhibited cell proliferation and invasion in renal cell carcinoma partially by increasing the expression of PTEN to inactivate P13K/AKT/mTOR signaling (Deng et al., 2018). Scutellarin was reported as a potential sensitizer to cisplatin treatment in ovarian cancer via strengthening the ability of cisplatin binding to DNA (Xie et al., 2019). Tang *et al.* showed that scutellarin could suppress cell metastasis and chemoresistance in glioma *in vitro* (Tang et al., 2019). Nevertheless, the specific molecular mechanisms of scutellarin involved in GBM are far from being completely understood.

According to CytoNCA analysis in PPI network, we found that the top 10 candidate targets of scutellarin against GBM were ALB, EGFR, SRC, HSP90AA1, ESR1, RHOA, IGF1, GSK3B, RAF1 and MDM2. GO and KEGG enrichment analysis disclosed that scutellarin might affect cell apoptosis and proliferation by modulating PI3K-AKT signaling pathway by targeting these key targets. By using MCODE plugin in Cytoscape, the core targets of module 1 and module 2 were possibly involved in apoptosis, DNA replication and cell proliferation by regulating PI3K-AKT and Ras signaling pathways. Through TCGA and molecular docking analysis, the suppressive role of scutellarin in GBM may be mediated by EGFR and RAF1. Moreover, EGFR and RAF1 were found as the hub genes associated with PI3K-AKT signaling.

EGFR, a member of the ERBB family of receptor tyrosine kinases, is often up-regulated in human carcinomas, and associated with the tumorigenesis and progression (Normanno et al., 2006).
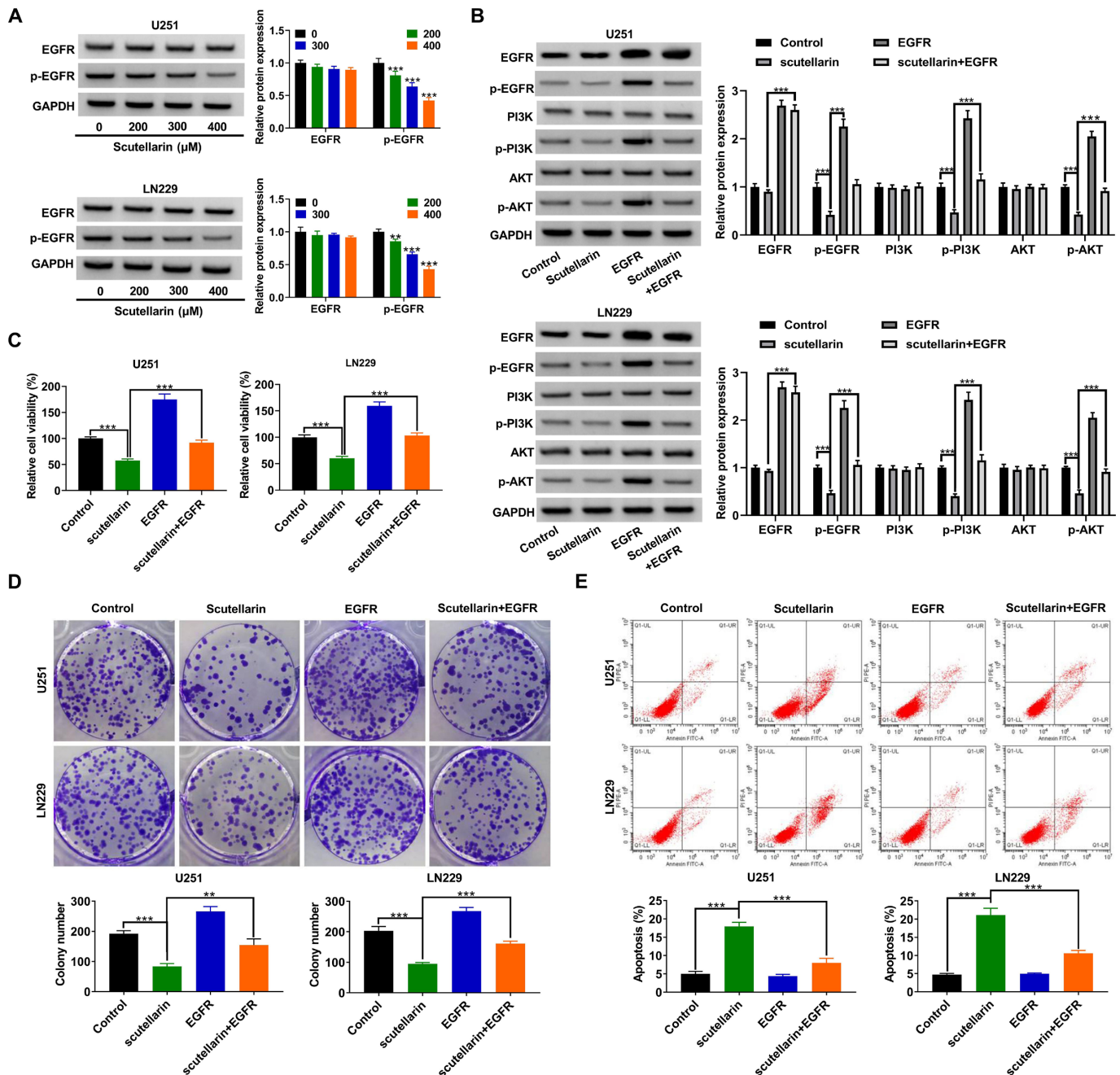
Figure 8. Scutellarin represses GBM cell proliferation and promotes apoptosis by inactivating EGFR/PI3K/AKT signaling pathway. (A) Western blot analysis of p-EGFR and EGFR in U251 and LN229 cells treated with scutellarin (0, 200, 300, and 400 μM) for 48 h. (B-E) U251 and LN229 transfected with EGFR (pcDNA-EGFR) were treated with or without 400 μM scutellarin for 48, followed by western blot assays of p-EGFR, EGFR, p-PI3K, PI3K, p-AKT and AKT (B), CCK-8 assays of cell viability (C), colony formation assay (D), and and flow cytometry assays of apoptosis (E). **$P < 0.01$, ***$P < 0.001$ vs. Control or scutellarin group.

Aberrant expression of EGFR can activate downstream pro-oncogenic signaling pathways, including PI3K-AKT pathways (Wee & Wang, 2017). Activation of PI3K/AKT pathway is always observed in human cancers, and is linked to cellular transformation, tumorigenesis, cancer progression, and drug resistance (Mayer & Arteaga, 2016). EGFR-PI3K-AKT signaling pathway has been proven to be involved in cancer cell proliferation and metastasis (Zhangyuan et al., 2020; Zheng et al., 2019). A

in silico analysis also eluciated the crucial roles of EGFR-PI3K-AKT-mTOR pathway in the tumorigenesis of diffuse brain gliomas (Brlek et al., 2021). Subsequent function experiments revealed that scutellarin suppressed cell proliferation, colony formation and enhanced apoptosis in a dose-dependent manner. Interestingly, scutellarin resulted in the increase of p-EGFR expression in a dose-dependent manner. These data suggested that scutellarin inhibited GBM progression and inactivated EGFR

signaling. Moreover, scutellarin-mediated inactivation of PI3K-AKT signaling was reversed in GBM cells after overexpressing EGFR. Furthermore, the inhibitory effects of scutellarin on cell malignant phenotypes were attenuated by EGFR overexpression. Combining these data together, we concluded that scutellarin repressed cell proliferation and enhanced apoptosis in GMB through inactivating EGFR-PI3K-AKT signaling. However, further animal models were required to confirm the functions and mechanisms of scutellarin in GBM *in vivo*.

In conclusion, we used network pharmacology method and molecular docking technology to investigate the possible targets and pharmacological mechanisms of scutellarin against GBM. Our finndings revealed that scutellarin suppressed GBM cell proliferation and induced apoptosis by targeting EGFR to inactivate PI3K-AKT signaling pathway. This study provides a theoretical basis for exploiting scutellarin as a clinical drug to fight against GBM.

Conflict of interest

No conflict of interests to be declared.

References

Abbas, M. N., Kausar, S., & Cui, H. (2020). Therapeutic potential of natural products in glioblastoma treatment: targeting key glioblastoma signaling pathways and epigenetic alterations. *Clinical & Translational Oncology*, 22(7), 963-977. http://dx.doi.org/10.1007/s12094-019-02227-3. PMid:31630356.

Babicki, S., Arndt, D., Marcu, A., Liang, Y., Grant, J. R., Maciejewski, A., & Wishart, D. S. (2016). Heatmapper: web-enabled heat mapping for all. *Nucleic Acids Research*, 44(W1), W147-W153. http://dx.doi.org/10.1093/nar/gkw419. PMid: 27190236.

Brlek, P., Kafka, A., Bukovac, A., & Pećina-Šlaus, N. (2021). Integrative cBioPortal analysis revealed molecular mechanisms that regulate EGFR-PI3K-AKT-mTOR pathway in diffuse gliomas of the brain. *Cancers (Basel)*, 13(13), 3247. http://dx.doi.org/10.3390/cancers13133247. PMid:34209611.

Chen, B., Chen, C., Zhang, Y., & Xu, J. (2021). Recent incidence trend of elderly patients with glioblastoma in the United States, 2000-2017. *BMC Cancer*, 21(1), 54. http://dx.doi.org/10.1186/s12885-020-07778-1. PMid:33430813.

Clough, E., & Barrett, T. (2016). The Gene Expression Omnibus Database. *Methods in Molecular Biology (Clifton, N.J.)*, 1418, 93-110. http://dx.doi.org/10.1007/978-1-4939-3578-9_5. PMid: 27008011.

Daina, A., Michielin, O., & Zoete, V. (2019). SwissTargetPrediction: updated data and new features for efficient prediction of protein targets of small molecules. *Nucleic Acids Research,* 47(W1), W357-W364. http://dx.doi.org/10.1093/nar/gkz382. PMid: 31106366.

Davis, M. E. (2016). Glioblastoma: overview of disease and treatment. *Clinical Journal of Oncology Nursing*, 20(5, Suppl), S2-S8. http://dx.doi.org/10.1188/16.CJON.S1.2-8. PMid:27668386.

Delgado-López, P. D., & Corrales-García, E. M. (2016). Survival in glioblastoma: a review on the impact of treatment modalities. *Clinical & Translational Oncology*, 18(11), 1062-1071. http://dx.doi.org/10.1007/s12094-016-1497-x. PMid:26960561.

Deng, W., Han, W., Fan, T., Wang, X., Cheng, Z., Wan, B., & Chen, J. (2018). Scutellarin inhibits human renal cancer cell proliferation and migration via upregulation of PTEN. *Biomedicine and Pharmacotherapy*, 107, 1505-1513. http://dx.doi.org/10.1016/j.biopha.2018.08.127. PMid:30257368.

Dutta, S., Mahalanobish, S., Saha, S., Ghosh, S., & Sil, P. C. (2019). Natural products: An upcoming therapeutic approach to cancer. *Food and Chemical Toxicology*, 128, 240-255. http://dx.doi.org/10.1016/j.fct.2019.04.012. PMid:30991130.

Erices, J. I., Torres, Á., Niechi, I., Bernales, I., & Quezada, C. (2018). Current natural therapies in the treatment against glioblastoma. *Phytotherapy Research*, 32(11), 2191-2201. http://dx.doi.org/10.1002/ptr.6170. PMid:30109743.

Hanachi, P., Hosseinpour, M., Bathaie, S., & Zarringhalami, R. (2020). Anticancer effect of Fumaria vaillanti extracts on BT-474 and MDA-MB-123 breast cancer cells. *Food Science and Technology (Campinas)*, 17(100), 57-66. http://dx.doi.org/10.52547/fsct.17.100.57.

Hao, C., & Xiao, P. G. (2014). Network pharmacology: a Rosetta Stone for traditional Chinese medicine. *Drug Development Research*, 75(5), 299-312. http://dx.doi.org/10.1002/ddr.21214. PMid:25160070.

Hou, L., Chen, L., & Fang, L. (2017). Scutellarin Inhibits proliferation, invasion, and tumorigenicity in human breast cancer cells by regulating HIPPO-YAP signaling pathway. *Medical Science Monitor*, 23, 5130-5138. http://dx.doi.org/10.12659/MSM.904492. PMid:29079722.

Huang, D. W., Sherman, B. T., Tan, Q., Kir, J., Liu, D., Bryant, D., Guo, Y., Stephens, R., Baseler, M. W., Lane, H. C., & Lempicki, R. A. (2007). DAVID Bioinformatics Resources: expanded annotation database and novel algorithms to better extract biology from large gene lists. *Nucleic Acids Research,* 35(suppl_2), W169-W175. http://dx.doi.org/10.1093/nar/gkm415. PMid:17576678.

Huang, T., Yang, X. K., Ji, J. L., Wang, Q. H., Wang, H. Y., & Dong, Z. (2019). Inhibitory effects of tanshinone IIA from Salvia miltiorrhiza Bge on human bladder cancer BIU-87 cells and xenograft in nude mice. *Food Science and Technology (Campinas)*, 40(1), 209-214. http://dx.doi.org/10.1590/fst.38818.

Kibble, M., Saarinen, N., Tang, J., Wennerberg, K., Mäkelä, S., & Aittokallio, T. (2015). Network pharmacology applications to map the unexplored target space and therapeutic potential of natural products. *Natural Product Reports*, 32(8), 1249-1266. http://dx.doi.org/10.1039/C5NP00005J. PMid:26030402.

Li, C. Y., Wang, Q., Wang, X., Li, G., Shen, S., & Wei, X. (2019). Scutellarin inhibits the invasive potential of malignant melanoma cells through the suppression epithelial-mesenchymal transition and angiogenesis via the PI3K/Akt/mTOR signaling pathway. *European Journal of Pharmacology*, 858, 172463. http://dx.doi.org/10.1016/j.ejphar.2019.172463. PMid:31211986.

Li, F., Wang, S., & Niu, M. (2021). Scutellarin inhibits the growth and EMT of gastric cancer cells through regulating PTEN/PI3K pathway. *Biological & Pharmaceutical Bulletin*, 44(6), 780-788. http://dx.doi.org/10.1248/bpb.b20-00822. PMid:34078809.

Liu, F., Zu, X., Xie, X., Zhang, Y., Liu, K., Chen, H., Wang, T., Bode, A. M., Dong, Z., & Kim, D. J. (2019a). Scutellarin suppresses patient-derived xenograft tumor growth by directly targeting AKT in esophageal squamous cell carcinoma. *Cancer Prevention Research (Philadelphia, Pa.)*, 12(12), 849-860. http://dx.doi.org/10.1158/1940-6207.CAPR-19-0244. PMid:31554627.

Liu, K., Tian, T., Zheng, Y., Zhou, L., Dai, C., Wang, M., Lin, S., Deng, Y., Hao, Q., Zhai, Z., & Dai, Z. (2019b). Scutellarin inhibits proliferation and invasion of hepatocellular carcinoma cells via down-regulation of JAK2/STAT3 pathway. *Journal of Cellular and Molecular Medicine*, 23(4), 3040-3044. http://dx.doi.org/10.1111/jcmm.14169. PMid:30697962.

Lv, W. L., Liu, Q., An, J. H., & Song, X. Y. (2019). Scutellarin inhibits hypoxia-induced epithelial-mesenchymal transition in bladder

cancer cells. *Journal of Cellular Physiology*, 234(12), 23169-23175. http://dx.doi.org/10.1002/jcp.28883. PMid:31127618.

Mayer, I. A., & Arteaga, C. L. (2016). The PI3K/AKT pathway as a target for cancer treatment. *Annual Review of Medicine*, 67(1), 11-28. http://dx.doi.org/10.1146/annurev-med-062913-051343. PMid:26473415.

Normanno, N., De Luca, A., Bianco, C., Strizzi, L., Mancino, M., Maiello, M. R., Carotenuto, A., De Feo, G., Caponigro, F., & Salomon, D. S. (2006). Epidermal growth factor receptor (EGFR) signaling in cancer. *Gene*, 366(1), 2-16. http://dx.doi.org/10.1016/j.gene.2005.10.018. PMid:16377102.

Ostrom, Q. T., Gittleman, H., Liao, P., Vecchione-Koval, T., Wolinsky, Y., Kruchko, C., & Barnholtz-Sloan, J. S. (2017). CBTRUS Statistical Report: primary brain and other central nervous system tumors diagnosed in the United States in 2010-2014. *Neuro-oncology*, 19(Suppl 5), v1-v88. http://dx.doi.org/10.1093/neuonc/nox158.

Peng, Y., Chen, F., Li, S. L., Liu, X., Wang, C., Yu, C. N., & Li, W. B. (2020). Tumor-associated macrophages as treatment targets in glioma. *Brain Science Advances*, 6(4), 306-323. http://dx.doi.org/10.26599/BSA.2020.9050015.

Sun, C., Li, C., Li, X., Zhu, Y., Su, Z., Wang, X., He, Q., Zheng, G., & Feng, B. (2018). Scutellarin induces apoptosis and autophagy in NSCLC cells through ERK1/2 and AKT Signaling Pathways in vitro and in vivo. *Journal of Cancer*, 9(18), 3247-3256. http://dx.doi.org/10.7150/jca.25921. PMid:30271483.

Szklarczyk, D., Morris, J. H., Cook, H., Kuhn, M., Wyder, S., Simonovic, M., Santos, A., Doncheva, N. T., Roth, A., Bork, P., Jensen, L. J., von Mering, C. (2017). The STRING database in 2017: quality-controlled protein–protein association networks, made broadly accessible. *Nucleic Acids Research, 45*(D1), D362-D368. http://dx.doi.org/10.1093/nar/gkw937. PMid: 27924014.

Tang, S. L., Gao, Y. L., & Hu, W. Z. (2019). Scutellarin inhibits the metastasis and cisplatin resistance in glioma cells. *OncoTargets and Therapy*, 12, 587-598. http://dx.doi.org/10.2147/OTT.S187426. PMid:30697056.

Thakkar, J. P., Dolecek, T. A., Horbinski, C., Ostrom, Q. T., Lightner, D. D., Barnholtz-Sloan, J. S., & Villano, J. L. (2014). Epidemiologic and molecular prognostic review of glioblastoma. *Cancer Epidemiology, Biomarkers & Prevention*, 23(10), 1985-1996. http://dx.doi.org/10.1158/1055-9965.EPI-14-0275. PMid:25053711.

Tykocki, T., & Eltayeb, M. (2018). Ten-year survival in glioblastoma. A systematic review. *Journal of Clinical Neuroscience*, 54, 7-13. http://dx.doi.org/10.1016/j.jocn.2018.05.002. PMid:29801989.

Vengoji, R., Macha, M. A., Batra, S. K., & Shonka, N. A. (2018). Natural products: a hope for glioblastoma patients. *Oncotarget*, 9(31), 22194-22219. http://dx.doi.org/10.18632/oncotarget.25175. PMid:29774132.

Wang, L., & Ma, Q. (2018). Clinical benefits and pharmacology of scutellarin: A comprehensive review. *Pharmacology & Therapeutics*, 190, 105-127. http://dx.doi.org/10.1016/j.pharmthera.2018.05.006. PMid:29742480.

Wang, X., Shen, Y., Wang, S., Li, S., Zhang, W., Liu, X., Lai, L., & Li, H. (2017). PharmMapper 2017 update: a web server for potential drug target identification with a comprehensive target pharmacophore database. *Nucleic Acids Research*, 45(W1), W356-W360. http://dx.doi.org/10.1093/nar/gkx374. PMid: 28472422.

Wee, P., & Wang, Z. (2017). Epidermal growth factor receptor cell proliferation signaling pathways. *Cancers (Basel)*, 9(5), 52. http://dx.doi.org/10.3390/cancers9050052. PMid:28513565.

Xie, Z., Guo, Z., Lei, J., & Yu, J. (2019). Scutellarin synergistically enhances cisplatin effect against ovarian cancer cells through enhancing the ability of cisplatin binding to DNA. *European Journal of Pharmacology*, 844, 9-16. http://dx.doi.org/10.1016/j.ejphar.2018.11.040. PMid:30503360.

Xiong, L. L., Du, R. L., Xue, L. L., Jiang, Y., Huang, J., Chen, L., Liu, J., & Wang, T. H. (2020). Anti-colorectal cancer effects of scutellarin revealed by genomic and proteomic analysis. *Chinese Medicine*, 15(1), 28. http://dx.doi.org/10.1186/s13020-020-00307-z. PMid:32226478.

Yao, Z. J., Dong, J., Che, Y. J., Zhu, M. F., Wen, M., Wang, N. N., Wang, S., Lu, A. P., Cao, D. S. (2016). TargetNet: a web service for predicting potential drug–target interaction profiling via multi-target SAR models. *Journal of Computer-Aided Molecular Design*, 30(5), 413-424. http://dx.doi.org/10.1007/s10822-016-9915-2. PMid:27167132.

Yuan, H., Ma, Q., Cui, H., Liu, G., Zhao, X., Li, W., & Piao, G. (2017). How can synergism of traditional medicines benefit from network pharmacology? *Molecules (Basel, Switzerland)*, 22(7), 1135. http://dx.doi.org/10.3390/molecules22071135. PMid:28686181.

Zanders, E. D., Svensson, F., & Bailey, D. S. (2019). Therapy for glioblastoma: is it working? *Drug Discovery Today*, 24(5), 1193-1201. http://dx.doi.org/10.1016/j.drudis.2019.03.008. PMid:30878561.

Zhangyuan, G., Wang, F., Zhang, H., Jiang, R., Tao, X., Yu, D., Jin, K., Yu, W., Liu, Y., Yin, Y., Shen, J., Xu, Q., Zhang, W., & Sun, B. (2020). VersicanV1 promotes proliferation and metastasis of hepatocellular carcinoma through the activation of EGFR–PI3K–AKT pathway. *Oncogene*, 39(6), 1213-1230. http://dx.doi.org/10.1038/s41388-019-1052-7. PMid:31605014.

Zheng, H., Yang, Y., Hong, Y. G., Wang, M. C., Yuan, S. X., Wang, Z. G., Bi, F. R., Hao, L. Q., Yan, H. L., & Zhou, W. P. (2019). Tropomodulin 3 modulates EGFR-PI3K-AKT signaling to drive hepatocellular carcinoma metastasis. *Molecular Carcinogenesis*, 58(10), 1897-1907. http://dx.doi.org/10.1002/mc.23083. PMid:31313392.

Zhou, Y. S., Zhao, D., Jiang, X. J., An, W., Gao, X. P., & Ma, Q. Y. (2021). Qilian Huaji decoction exerts an anti-cancer effect on hepatocellular carcinoma by upregulating miR-122. *Food Science and Technology*. In press.